European Journal of Mechanics / A Solids 92 (2022) 104454

Contents lists available at ScienceDirect

European Journal of Mechanics / A Solids

journal homepage: www.elsevier.com/locate/ejmsol

Stochastic continuum approach to high-cycle fatigue: Modelling stress history as a stochastic process

Tero Frondelius [a,d], Terhi Kaarakka [b], Reijo Kouhia [c,*], Jari Mäkinen [c], Heikki Orelma [c], Joona Vaara [a]

[a] Wärtsilä Marine Solutions, R&D and Engineering, Järvikatu 2-4, 65100 Vaasa, Finland
[b] Tampere University, Unit of Computing Science/Mathematics, Korkeakoulunkatu 10, 33720 Tampere, Finland
[c] Tampere University, Unit of Civil Engineering, Structural Mechanics, Korkeakoulunkatu 10, 33720 Tampere, Finland
[d] University of Oulu, Erkki Koiso-Kanttilan katu 1, 90014, Oulu, Finland

ARTICLE INFO

Keywords:
High-cycle fatigue
Out-of-phase loading
Stochastic loading
Ornstein–Uhlenbeck process
Lifetime distribution
Safety factor distribution

ABSTRACT

In this article, the continuum-based high-cycle fatigue analysis method, introduced by Ottosen, Stenström and Ristinmaa in 2008, is extended to cases where the stress history is a stochastic process. The basic three-parameter Ornstein–Uhlenbeck process is chosen for stress description. As a practical example, the theory is applied in both finite and infinite life cases. A definition for the safety factor is introduced, which is reduced to a minimization problem of the value for the endurance surface. In the stochastic case, the values of the endurance surface form a stochastic process and the cumulative distribution function can be constructed for its maximum values.

1. Introduction

Mechanical fatigue phenomena occur when a material is subjected to the repeated application of stresses or strains, which produces changes in the material microstructure, initiation, growth and coalescence of microdefects, thus degrading the material properties, see Bolotin (1999), Suresh (1998), Murakami (2002) and Vaara et al. (2017). It is customary to distinguish between high-cycle (HCF) and low-cycle fatigue (LCF). In low-cycle fatigue, plastic deformations occur at the macroscopic scale, while when the loading is in the high-cycle fatigue regime, the macroscopic behaviour can be considered primarily as elastic. If the loading consists of well-defined cycles, the transition between LCF and HCF regimes is typically considered to occur between 10^3 and 10^4 cycles.

In this study, only high-cycle fatigue is considered. Classical methods for HCF analysis can be broadly classified as stress invariant-, critical plane-, strain energy- and average stress based approaches. These approaches are well-defined if the loading consists of well-defined cycles. For arbitrary loading histories, they need the definition of an equivalent uniaxial loading cycle. Another deficiency is that heuristic damage accumulation rules have to be applied. To remove these shortcomings, Ottosen et al. (2008) proposed a continuum-based model where they postulated a moving endurance surface in the stress space where the movement and damage evolution are governed by properly formulated evolution equations. This *evolution equation-based continuum approach* to HCF is also used by Brighenti et al. (2012, 2013), Lindström et al. (2020) and Suresh et al. (2020, 2021), where this approach is called the *time continuous fatigue analysis method*. Extension to transverse isotropy is given in Holopainen et al. (2016b) and gradient effects are included in Ottosen et al. (2018). Recently, Lindström (2020) modified the original approach to improve the fatigue life predictions for non-proportional stress histories. In the evolution equation-based approach, the stress history need not to be stored when computing the fatigue life, which is a great advantage in large scale computations (Lilja et al., 2020).

Other continuum mechanics approach for high-cycle fatigue include the two scale models where scale transition from the micro-scale plasticity to the macro-scale is implemented using the Eshelby–Kröner localization law, see (Lemaitre and Desmorat, 2005, Section 6.2.3), (Desmorat et al., 2007; Mareau et al., 2013; Mareau and Morel, 2019).

Micro-mechanically motivated crystal plasticity models have been used especially in low-cycle fatigue analysis (Manonukul and Dunne, 2004; Grilli et al., 2015; Zhang et al., 2020), see also a recent overview by Abdul-Latif (2021).

There is inherently a stochastic nature to fatigue phenomena. The fatigue life has a characteristic scatter even under a constant cyclic loading. The Weibull weakest link theory Weibull (1939) has been used

* Corresponding author.
E-mail addresses: tero.frondelius@wartsila.com, tero.frondelius@oulu.fi (T. Frondelius), terhi.kaarakka@tuni.fi (T. Kaarakka), reijo.kouhia@tuni.fi (R. Kouhia), jari.makinen@tuni.fi (J. Mäkinen), heikki.orelma@tuni.fi (H. Orelma), joona.vaara@wartsila.com (J. Vaara).

https://doi.org/10.1016/j.euromechsol.2021.104454
Received 26 February 2021; Received in revised form 13 October 2021; Accepted 24 October 2021
Available online 6 November 2021

to describe the statistically distributed flaws and defects in the material that is reflected in the fatigue behaviour (Böhm and Heckel, 1982; Bomas et al., 1999; Flaceliere and Morel, 2004; Wormsen et al., 2007). Under real-life loading conditions there always exist random fluctuations, and thus the stress history can only be described by statistical distributions. For irregular loading histories, the classical method to predict a lifetime is the Rainflow method, which is based on a construction of an equivalent cycle. The method is essentially one-dimensional, but can be extended to the multiaxial case considering equivalent stress criteria. It could also be extended to a stochastic case, see Banvillet et al. (2004), Liu and Mahadevan (2007), see also Cristofori et al. (2011), Carpinteri et al. (2016), Wei et al. (2020). A comparison of classical "static" multiaxial fatigue models under random loading is presented in Portugal et al. (2019). A common process is to estimate the autocorrelation function from the obtained stress data, then the spectral density function can be found by using the fast Fourier transform, and the lifetime can be approximated with a level crossing formula, usually the so-called Rice's formula, see e.g. Kratz (2006).

The stochastic Rainflow method works best in one-dimensional cases, because the generalization to a multiaxial case is somewhat artificial. Considering only one equivalent stress process is a gross simplification. Another problem is that its generalization is difficult and limited. This paper describes a stochastic extension to the evolution equation-based multiaxial high-cycle fatigue model proposed by Ottosen et al. (2008), which is applicable for arbitrary loading histories and treats the fatigue phenomenon as a process and not as a specific state of cyclic stress causing fatigue.

2. Continuum-based fatigue model

Ottosen et al. (2008) proposed a continuum approach for HCF modelling which is based on a moving endurance surface and a set of internal variables characterizing its movement and damage. Change of these internal variables is governed by evolution equations. Such an approach treats multiaxial stress states and arbitrary loading sequences in a unified manner, and the heuristic cycle-counting techniques are not needed.

The original form of the endurance surface proposed in Ottosen et al. (2008) for isotropic high-cycle fatigue has the following form

$$\beta = \frac{1}{\sigma_{\mathrm{oe}}}(\bar{\sigma} + AI_1 - \sigma_{\mathrm{oe}}) = 0, \tag{1}$$

where I_1 is the first invariant of the stress tensor $\boldsymbol{\sigma}$, i.e. $I_1 = \operatorname{tr}\boldsymbol{\sigma}$, and the effective stress $\bar{\sigma}$ is defined by the second invariant of the reduced deviatoric stress $\boldsymbol{s} - \boldsymbol{\alpha}$ as

$$\bar{\sigma} = \sqrt{3J_2(\boldsymbol{s} - \boldsymbol{\alpha})} = \sqrt{\tfrac{3}{2}\operatorname{tr}(\boldsymbol{s} - \boldsymbol{\alpha})^2}. \tag{2}$$

The deviatoric stress tensor is $\boldsymbol{s} = \boldsymbol{\sigma} - \frac{1}{3}\operatorname{tr}(\boldsymbol{\sigma})\boldsymbol{I}$, where $\boldsymbol{I}$ stands for the identity tensor.

Brighenti et al. (2012, 2013) used a more complicated form for the endurance surface, which can result in a better fit to the experiments. However, the simple interpretation of the model parameters is lost and the estimation of model parameters is more involved.

It is shown in Ottosen et al. (2008, Section 4) that in the special case of uniaxial cyclic loading, where the stress varies between $\sigma_{\mathrm{m}} - \sigma_{\mathrm{a}}$ and $\sigma_{\mathrm{m}} + \sigma_{\mathrm{a}}$, a linear relation between the mean stress and amplitude, i.e. a linear Haigh diagram, $\sigma_{\mathrm{a}} + A\sigma_{\mathrm{m}} - \sigma_{\mathrm{oe}} = 0$, is obtained. As it can be noticed, the non-dimensional positive parameter A is the opposite value of the slope in the Haigh diagram and σ_{oe} equals the fatigue limit σ_{-1} in the fully reversed loading case. Thus, A can be determined, e.g. using the formula $A = (\sigma_{-1}/\sigma_0) - 1$, where σ_0 is the fatigue limit amplitude for tensile pulsating loading.

Brighenti et al. (2012, 2013) used a more complex form for the endurance surface. This makes the interpretation of the model parameters more difficult and the parameter estimation more involved. Genetic algorithms were used for parameter estimation in Brighenti et al. (2012).

A back stress-like deviatoric tensor $\boldsymbol{\alpha}$ is a history variable. Its movement determines the movement of the endurance surface (1) in the stress space. The physical meaning of the $\boldsymbol{\alpha}$-tensor in the infinite life regime is possibly linked to microscale plasticity. Solution problem for the stationary value of the $\boldsymbol{\alpha}$-tensor (14) is identical to the shakedown minmax-problem for solution of the plastic strain, see e.g. Polizzotto et al. (2001), Nguyen (2003). When applied to cases more close to the low-cycle regime, it might contain information from macroscale plasticity too. However, in the true low-cycle fatigue due to the mean stress relaxation the influence of the Bauschinger effect is decreasing. Evolution of the deviatoric $\boldsymbol{\alpha}$-tensor is governed by the evolution equation

$$\dot{\boldsymbol{\alpha}} = C(\boldsymbol{s} - \boldsymbol{\alpha})\dot{\beta}, \tag{3}$$

where C is a positive dimensionless material parameter and the superimposed dot denotes time rate. The shape of the endurance surface (1) in the deviatoric plane is circular and the meridian lines are straight, as with the case of the Drucker–Prager model in plasticity, see Figs. 1 and 2. The explicit form for the time differentiation of β is

$$\dot{\beta} = \frac{1}{\sigma_{-1} + C\bar{\sigma}}\left(\frac{3}{2}\frac{(\mathbf{s} - \boldsymbol{\alpha})}{\bar{\sigma}} + A\boldsymbol{I}\right) : \dot{\boldsymbol{\sigma}},$$

where : denotes the double dot product between second order tensors, i.e. $\boldsymbol{A} : \boldsymbol{B} = \operatorname{tr}(\boldsymbol{A}\boldsymbol{B}^{\mathrm{T}})$. In the model, all the stress tensors $\boldsymbol{\sigma}$, $\mathbf{s}$ and $\boldsymbol{\alpha}$ are functions of space and time. Since gradient effects are not considered in this paper, the variation of stress at some fixed point is of particular interest. For this reason, we can think that the stress depends only on time, i.e. geometrically they are curves $\boldsymbol{\sigma}(t)$, $\mathbf{s}(t)$ and $\boldsymbol{\alpha}(t)$ in a stress space associated with a point of the body.

Fatigue damage is modelled by using an isotropic damage variable function D taking values in $[0, 1]$, for which the evolution is given in the form

$$\dot{D} = \frac{K}{(1 - D)^k}\exp(L\beta)\dot{\beta} \tag{4}$$

where $K > 0$, $L > 0$ and $k \geq 0$ are material parameters. Since damage never decreases, i.e. $\dot{D} \geq 0$, it then follows that damage evolution takes place only when $\dot{\beta} \geq 0$. The *life or failure time* T_{f} is the time when the damage variable attains the value one, i.e. $D(T_{\mathrm{f}}) = 1$. In contrast to rate-independent plasticity, the stress state can lie outside the endurance surface. When the stress state is outside the endurance surface and moves away from this surface the evolution of the $\boldsymbol{\alpha}$-tensor and damage takes place

$$\beta \geq 0 \quad \text{and} \quad \dot{\beta} > 0, \tag{5}$$

see Fig. 1.

The damage variable D try to indicate the damage, which accumulates in the microscopical scale near surface intrusions/extrusions, voids and inclusions inside the material. It is not coupled to the constitutive behaviour thus facilitating also easy post-processing HCF-analysis.

Originally in Ottosen et al. (2008), the value $k = 0$ was used. It means that in a constant amplitude cyclic loading, the damage increase per cycle will saturate to a constant value. However, in reality the damage rate increases with increasing damage and an alternative formulation with $k = 1$ is used in Holopainen et al. (2016b). In that case, i.e. $k \geq 0$, the damage rate per cycle increases with increasing damage, see the results in Holopainen et al. (2016a, Figures 6 and 7).

Although the parameter k results in a non-linear damage evolution, it has no effect to the fatigue life in a two-step loading, i.e. it results in the linear Palmgren–Miner damage accumulation law irrespective of the value of k. This could indirectly be seen also in the derivation given by Suresh et al. (2020). If k is changed, then only parameter K need to be changed to obtain the same SN-curve. For instance in Ottosen et al. (2008) the parameters are calibrated to the SAE4340 steel with $k = 0$

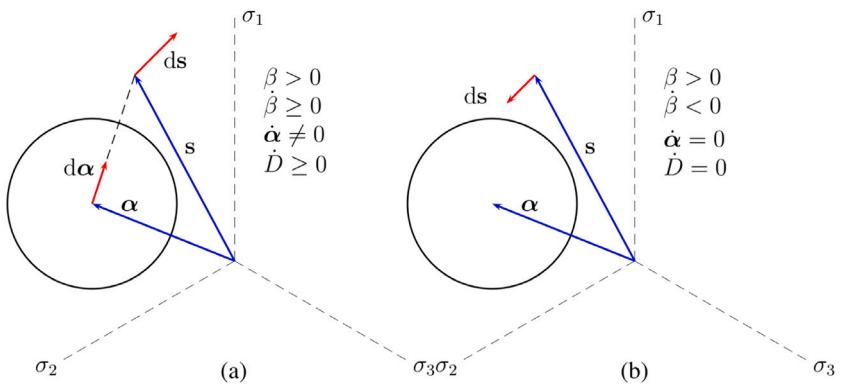

Fig. 1. (a) Movement of the endurance surface and damage growth occur when the stress is outside the endurance surface and moving away from it. (b) When the stress is outside the endurance surface but the stress increment is directed towards the endurance surface, damage and back stress does not evolve.

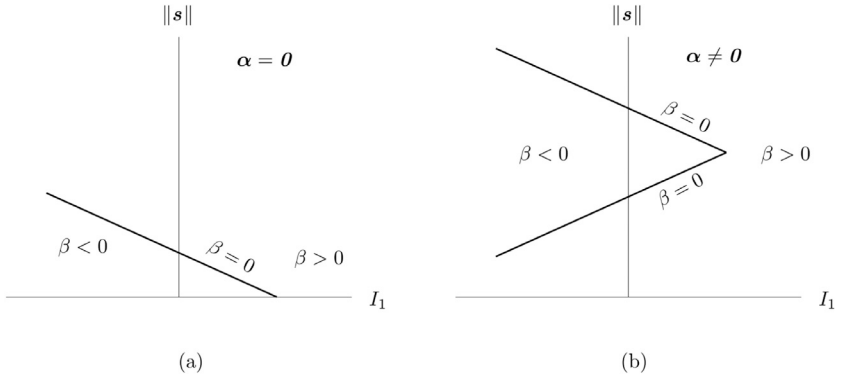

Fig. 2. Endurance surface presented in a meridian plane as the backstress is (a) $\boldsymbol{\alpha} = \boldsymbol{0}$ and (b) $\boldsymbol{\alpha} \neq \boldsymbol{0}$.

resulting in $K = 2.65 \cdot 10^{-5}$. If k is changed to $k = 1$ or 2, the value of K changes to $K = 1.325 \cdot 10^{-5}$ or $8.835 \cdot 10^{-6}$, respectively.

The behaviour of the model for various loading cases has been demonstrated in Ottosen et al. (2008), Holopainen et al. (2016b) including the mean stress effect, the phase shift and phase difference effects (between two normal stresses and between a normal stress and a shear stress). Qualitatively and quantitatively the mode responses are in accordance to the experimental findings. In variable amplitude loading the model with a constant k results in a linear Palmgren–Miner damage accumulation rule. However, if the parameter k depends on the stress state, like

$$k(\beta) = k_0 \exp(-k_1 \beta), \tag{6}$$

where k_0 and k_1 are dimensionless parameters a non-linear damage accumulation in a two-level cyclic test is obtained. The parameter k_1 then controls the deviation from the linear damage accumulation.

To demonstrate that by selecting the parameter values as $k_0 = 2$ and $k_1 = 10$, and calibrating the other parameters to the SAE 4340 steel SN-curve given in Ottosen et al. (2008), the following values are obtained

$$A = 0.225, \quad C = 1.35, \quad K = 1.05 \cdot 10^{-5}, \quad L = 17.8.$$

In a two-level fully reversed cyclic normal stress test with the highest amplitude of $1.3\sigma_{-1}$ and the lowest either $1.2\sigma_{-1}$ or $1.1\sigma_{-1}$, the results are shown in Fig. 3. The results are in a qualitative agreement of the experimental findings that a high-amplitude loading followed by a low-amplitude loading is more damaging than loading in the opposite order. If compared to the model by Chaboche and Lesne (1988), the present model results in milder non-linearity. However, the linear accumulation is usually considered to be adequate in random fatigue analysis.

For two level loading with a normal and shear stress the model predictions are shown in Fig. 4. They are qualitatively in accordance to the results presented in Kalluri and Bonacuse (2000).

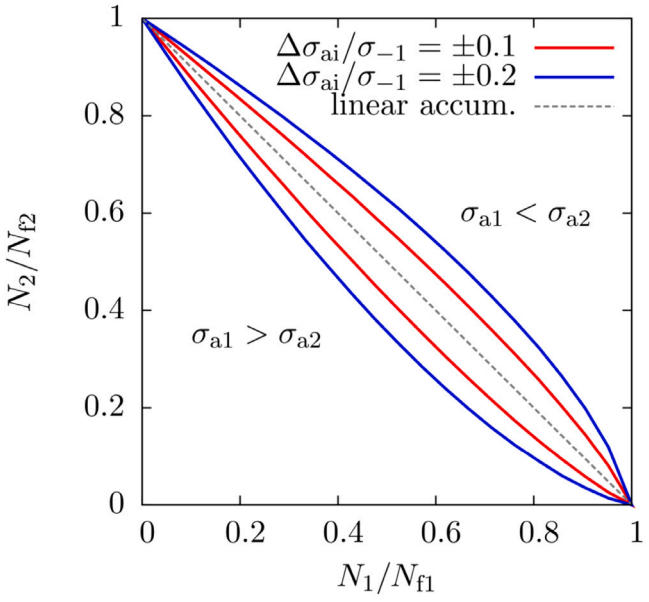

Fig. 3. Two-level cyclic normal stress loading with $R = -1$.

3. Stochastic approach to continuum-based fatigue model

The deterministic continuum-based fatigue model, described in the preceding section, is mathematically based on differential equations. A natural step further is to consider these equations as stochastic

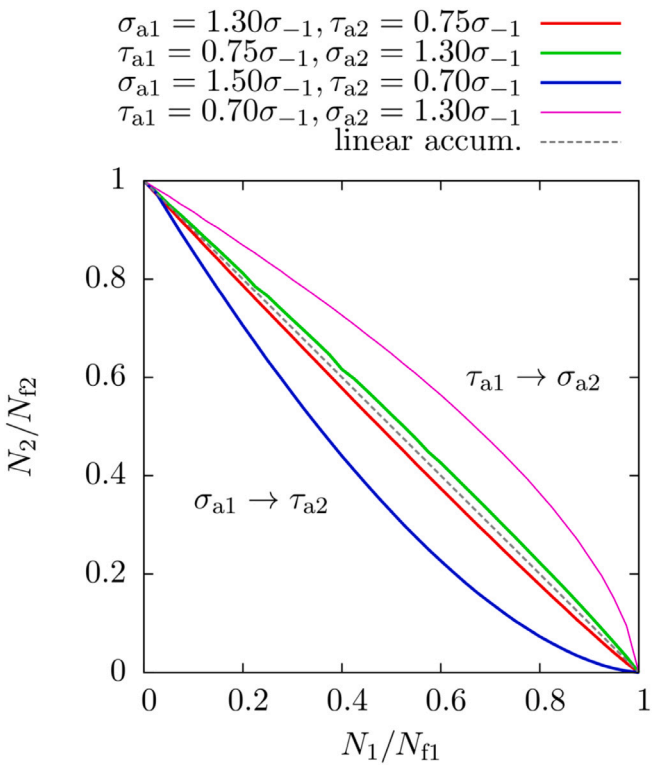

Fig. 4. Two-sequence fully reversed cyclic normal and shear loading.

differential equations, and this observation opens the way to formulate the whole theory in the context of stochastic analysis.

It is assumed that the reader is familiar with the basics of probability theory, stochastic processes and stochastic differential equations, e.g. Lindgren (2013), Sobczyk (1991).

To obtain a stochastic formulation, we assume that $\boldsymbol{\sigma}(t)$, $\boldsymbol{\alpha}(t)$ and $D(t)$ are continuous stochastic processes, where $t \geq 0$ is a real parameter. To be more precise, the first two are tensor-valued stress processes, i.e. time-depended random variables defined in a probability space $(\Omega, \Gamma, \mathbb{P})$, where Ω is a set containing all possible outcomes, Γ is a set of events and $\mathbb{P}$ is a function relating events to probabilities. In practice, this probability space is hard to define explicitly. Usually it is enough to assume that time point-wise distributions of stochastic processes are Gaußians. Hence, we may ignore the question about probability space.

In this paper, we assume that the stress process $\boldsymbol{\sigma}(t)$ is given. Usual choices for proper stochastic processes are so-called ergodic processes, see e.g. Lindgren (2013).

Let us consider computed or measured stress data $\widetilde{\boldsymbol{\sigma}}_0, \widetilde{\boldsymbol{\sigma}}_1, \ldots, \widetilde{\boldsymbol{\sigma}}_n$ recorded at the time instants $t_0, t_1, \ldots, t_n$ in $[0, T]$. The fundamental problem is to find a stochastic stress process $\boldsymbol{\sigma}(t)$ such that the stress data may be seen as an approximation for realizations of the process.

When the stress process $\boldsymbol{\sigma}(t)$ is fixed using some methods, we simply proceed as follows. In the deterministic case, the lifetime T_f for given stress history $\boldsymbol{\sigma}(t)$ is defined via the equation $D(T_f) = 1$ and it is a real number. In the stochastic case, we solve the system for various realizations of the process $\boldsymbol{\sigma}(t)$ and obtain the distribution of life times. Hence, the lifetime T_f is a random variable. In real life, this is of course more realistic. After the next section, we will discuss more what kind of different possibilities we have to use it in applications.

4. Periodic stress history with a stationary noise

It is now assumed that the stress process can be divided as

$$\boldsymbol{\sigma}(t) = \boldsymbol{\sigma}_p(t) + \boldsymbol{\sigma}_n(t), \tag{7}$$

where $\boldsymbol{\sigma}_p(t)$ is the deterministic part of the stress and $\boldsymbol{\sigma}_n(t)$ is the noise part. The deterministic part $\boldsymbol{\sigma}_p(t)$ is assumed to be a function and $\boldsymbol{\sigma}_n(t)$ a stationary stochastic process. Hence, if $\widetilde{\boldsymbol{\sigma}}(t)$ is a recorded realization of the process, we may compute a realization for noise as

$$\widetilde{\boldsymbol{\sigma}}_n(t) = \widetilde{\boldsymbol{\sigma}}(t) - \boldsymbol{\sigma}_p(t),$$

and using the estimation method, we may construct a noise process $\boldsymbol{\sigma}_n(t)$. In this section, we assume that the noise is an Ornstein–Uhlenbeck process, which is a well-known and easily handled stationary stochastic process. See also Kaleva and Orelma (2021) for another model for the stochastic part.

4.1. Noise stress process as an Ornstein–Uhlenbeck process

To simplify the notation, we drop the subscript n indicating the noise contribution of the stress process. A one-dimensional Ornstein–Uhlenbeck process is usually given as a stochastic differential equation[1]

$$d\sigma(t) = \lambda(\mu - \sigma(t))dt + \eta dW(t). \tag{8}$$

The process is a stationary Gauß-Markov process depending on three parameters $\lambda > 0$, μ and $\eta > 0$, and the process tends to drift towards its long-term mean. In (8), $W(t)$ denotes the Brownian motions or Wiener processes. The Wiener process $W(t)$ represents Gaußian white noise, which describes in our case random fluctuation of the stress. The parameter η describes the size of the fluctuation and together with the Wiener process, the term $\eta dW(t)$ is called the "white noise" and $\lambda(\mu - \sigma(t))dt$ the "mean reverting" or "drift" term. Here, λ describes how strongly the system reacts to perturbations, and μ is the asymptotic mean of the process.

Solution of the stochastic differential Eq. (8) can be written as, see e.g. Gardiner (1997)

$$\sigma(t) = \mu + (\sigma_0 - \mu)e^{-\lambda t} + \eta \int_0^t e^{-\lambda(t-s)} dW(s). \tag{9}$$

The integral term of the preceding formula is the so-called Itô integral with respect to the Wiener process, see e.g. Sobczyk (1991), Kloeden and Platen (1992), and $\sigma(0) = \sigma_0$ is an initial condition of the process. From the formula (9), we obtain the conditional expectation

$$\mathrm{E}[\sigma_n(t) : \sigma(0) = \sigma_0] = \mu + (\sigma_0 - \mu)e^{-\lambda t} \tag{10}$$

and the variance

$$\mathrm{Var}[\sigma(t) : \sigma(0) = \sigma_0] = \frac{\eta^2}{2\lambda}(1 - e^{-2\lambda t}). \tag{11}$$

In the sequel, we use the Voigt notation for the symmetric tensors $\boldsymbol{\sigma}$ and $\boldsymbol{\alpha}$, i.e. they are considered as 6-dimensional vectors. Hence, the present application of the Ornstein–Uhlenbeck process is a stochastic process with 18 parameters written in the vector form

$$d\boldsymbol{\sigma}(t) = \lambda(\boldsymbol{\mu} - \boldsymbol{\sigma}(t))dt + \boldsymbol{\eta} d\mathbf{W}(t),$$

where the Voigt notation is used for the stress

$$\boldsymbol{\sigma}(t) = \begin{bmatrix} \sigma_{11}(t) \\ \sigma_{22}(t) \\ \sigma_{33}(t) \\ \sigma_{12}(t) \\ \sigma_{23}(t) \\ \sigma_{13}(t) \end{bmatrix}, \quad \boldsymbol{\mu} = \begin{bmatrix} \mu_{11} \\ \mu_{22} \\ \mu_{33} \\ \mu_{12} \\ \mu_{23} \\ \mu_{13} \end{bmatrix}, \quad \mathbf{W}(t) = \begin{bmatrix} W_{11}(t) \\ W_{22}(t) \\ W_{33}(t) \\ W_{12}(t) \\ W_{23}(t) \\ W_{13}(t) \end{bmatrix}$$

and

$$\lambda = \mathrm{diag}(\lambda_{11}, \lambda_{22}, \lambda_{33}, \lambda_{12}, \lambda_{23}, \lambda_{13}), \quad \boldsymbol{\eta} = \mathrm{diag}(\eta_{11}, \eta_{22}, \eta_{33}, \eta_{12}, \eta_{23}, \eta_{13}).$$

[1] As usual, the standard "small d" notation for stochastic differential equations is used. The fundamental reason to use this notation is that the Wiener process $W(t)$ is nowhere differentiable, i.e. $dW(t)/dt$ does not exist, that is, it is impossible to use classical time differentiable notation. For more information, see e.g. Sobczyk (1991), Kloeden and Platen (1992). Notice that the unit of the Wiener process W is $\sqrt{\text{time}}$ and for η it is stress/$\sqrt{\text{time}}$.

4.2. Stochastic evolution equations

After fixing the form of the stress process, we may write the stochastic differential equation system, which describes the fatigue behaviour at the point. Considering $\boldsymbol{\alpha}(t)$ as a vector-valued stochastic process, we obtain the real valued stochastic processes $\beta(\boldsymbol{\alpha}(t), \boldsymbol{\sigma}(t))$ and $\dot{\beta}(\boldsymbol{\alpha}(t), \boldsymbol{\sigma}(t))$. As in (7), it is now assumed that the stress $\boldsymbol{\sigma}(t)$ can be additively decomposed, i.e.

$$\boldsymbol{\sigma}(t) = \boldsymbol{\sigma}_{\mathrm{p}}(t) + \boldsymbol{\sigma}_{\mathrm{n}}(t),$$

where the noise part $\boldsymbol{\sigma}_{\mathrm{n}}$ is an Ornstein–Uhlenbeck process. Then we need to solve the following stochastic differential equation system

$$d\boldsymbol{\alpha}(t) = \begin{cases} \dot{\beta}(\boldsymbol{\alpha}(t), \boldsymbol{\sigma}(t)) C(\mathbf{s}(t) - \boldsymbol{\alpha}(t)) dt, & \text{if } \beta > 0,\ \dot{\beta} > 0, \\ 0, & \text{otherwise,} \end{cases}$$

$$dD(t) = \begin{cases} K(1 - D(t))^{-k} \dot{\beta}(\boldsymbol{\alpha}(t), \boldsymbol{\sigma}(t)) e^{L\beta((\boldsymbol{\alpha}(t), \boldsymbol{\sigma}(t)))} dt, & \text{if } \beta > 0,\ \dot{\beta} > 0, \\ 0, & \text{otherwise.} \end{cases}$$

This is called the *stochastic evolution system*. The system consists of the *evolution equations for the back stress and damage*. In the next section, we will consider methods of how to find matrices $\boldsymbol{\lambda}$, $\boldsymbol{\mu}$ and $\boldsymbol{\eta}$ from a given noise.

4.3. On parameter estimation

Like we saw in the preceding section, we model the recorded noise data as an Ornstein–Uhlenbeck process

$$d\boldsymbol{\sigma}_{\mathrm{n}}(t) = \boldsymbol{\lambda}(\boldsymbol{\mu} - \boldsymbol{\sigma}_{\mathrm{n}}(t)) dt + \boldsymbol{\eta} d\mathbf{W}(t).$$

To calibrate this model to recorded data, we have two options, namely the calibration using least square regression and Maximum Likelihood estimates. The methods are well-known and in the Gaußian case they are the same. Without loss of generality, we can consider only a one-dimensional case since the components of the vector-valued process (8) are uncoupled.

Let $\widetilde{\sigma}_0, \widetilde{\sigma}_1, \dots, \widetilde{\sigma}_n$ be the recorded values of a stress on the time interval $[0, T]$. Let the corresponding recording times be $0 = t_0 < t_1 < \cdots < t_n = T$. Let $\sigma(t_0), \sigma(t_1), \dots, \sigma(t_n)$ be points of a corresponding sample of the stationary process (8). The problem is to find the parameters (μ, λ, η) such that the resulting process would describe the stochastic behaviour of the original recorded process as well as possible.

A well-known method of estimating the parameters of a statistical model is called the maximum likelihood estimation, and it governs the set of values of the model parameters that maximizes the so-called likelihood function. A reference for the theory is, e.g. James and Webber (2000), Pfanzagl (1994).

Since the Ornstein–Uhlenbeck process $\sigma(t)$ is Gaußian, the probability distribution function has the form

$$f_{\sigma(t)}(\tau; \mu, \lambda, \eta) = \frac{1}{\sqrt{2\pi\zeta(t; \sigma_0)}} e^{-\frac{(\tau - \epsilon(t;\sigma_0))^2}{2\zeta(t;\sigma_0)}}$$

where the expectational value $\epsilon(t; \sigma_0) = \mathrm{E}[\sigma(t) : \sigma(0) = \sigma_0]$ and the variance $\zeta(t; \sigma_0) = \mathrm{Var}[\sigma(t) : \sigma(0) = \sigma_0]$. Since the Ornstein–Uhlenbeck process is also a Markov process, the future depends only on the value and it is independent its past, we may compute the density function of the joint probability distribution of $\sigma(t_0), \sigma(t_1), \dots, \sigma(t_n)$ as

$$f_{\text{joint}}(\tau_0, \tau_1, \dots, \tau_n; \mu, \lambda, \eta) = f_{\sigma(t_0)}(\tau_0; \mu, \lambda, \eta) f_{\sigma(t_1)|\sigma(t_0)}(\tau_1; \mu, \lambda, \eta) \cdots f_{\sigma(t_n)|\sigma(t_{n-1})}(\tau_n; \mu, \lambda, \eta).$$

The *maximum likelihood principle* says that we need to find (μ, λ, η) such that the joint probability distribution takes its maximum subject to $\sigma(t_0) = \widetilde{\sigma}_0$, $\sigma(t_1) = \widetilde{\sigma}_1$, …, $\sigma(t_n) = \widetilde{\sigma}_n$. In other words, we determine the parameters such that the probability to get back the recorded values is the highest possible.

The Ornstein–Uhlenbeck process is a strictly stationary process, i.e. its statistical properties do not change by time. This means that the random vectors $(\sigma(t_0), \sigma(t_1), \dots, \sigma(t_n))$ and $(\sigma(t_0+t'), \sigma(t_1+t'), \dots, \sigma(t_n+t'))$ have the same distribution under a time shift t'. We denote the time increments by $\Delta t_j = t_j - t_{j-1}$. Due to stationarity, we may write the density functions in the form

$$\begin{aligned} &f_{\sigma(t_j)|\sigma(t_{j-1})}(\tau_j; \mu, \lambda, \eta) \\ &= \frac{1}{\sqrt{2\pi\zeta(\Delta t_j; \tau_{j-1})}} \exp\Big(-\frac{(\tau_j - \epsilon(\Delta t_j; \tau_{j-1}))^2}{2\zeta(\Delta t_j; \tau_{j-1})}\Big) \\ &= \frac{1}{\sqrt{\pi}} \frac{1}{\sqrt{\frac{\eta^2}{\lambda}\big(1 - e^{-2\lambda\Delta t_j}\big)}} \exp\Big(-\frac{\lambda\big(\tau_j - \mu - (\tau_{j-1} - \mu)e^{-\lambda\Delta t_j}\big)^2}{\eta^2\big(1 - e^{-2\lambda\Delta t_j}\big)}\Big) \end{aligned}$$

for $j = 1, \dots, n$ and $t_0 = 0$ we have

$$f_{\sigma(t_0)}(\tau_0; \mu, \lambda, \eta) = \frac{\sqrt{\lambda}}{\sqrt{\pi}\eta} e^{-\frac{\lambda(\tau_0 - \mu)^2}{\eta^2}}.$$

Then we may define the likelihood function

$$\begin{aligned} L(\mu, \lambda, \eta) &= f_{\sigma(t_0)}(\tau_0; \mu, \lambda, \eta) \prod_{j=1}^{n} f_{\sigma(t_j)|\sigma(t_{j-1})}(\widetilde{\sigma}_j; \mu, \lambda, \eta) \\ &= \Big(\frac{\lambda}{\pi\eta^2}\Big)^{\frac{n+1}{2}} e^{-\frac{\lambda(\tau_0 - \mu)^2}{\eta^2}} \prod_{j=1}^{n} \frac{\exp\left(-\frac{\lambda(\tau_j - \mu - (\tau_{j-1} - \mu)e^{-\lambda\Delta t_j})^2}{\eta^2(1 - e^{2\lambda\Delta t_j})}\right)}{\sqrt{1 - e^{-2\lambda\Delta t_j}}}. \end{aligned}$$

Since the process is Gaußian, it is easier to maximize the so-called log-likelihood function, defined by

$$\begin{aligned} K(\mu, \lambda, \eta) = \ln L(\mu, \lambda, \eta) &= \frac{n+1}{2} \ln\Big(\frac{\lambda}{\pi\eta^2}\Big) - \frac{\lambda(\tau_0 - \mu)^2}{\eta^2} \\ &- \frac{1}{2} \sum_{j=1}^{n} \ln(1 - e^{-2\lambda\Delta t_j}) \\ &- \frac{\lambda}{\eta^2} \sum_{j=1}^{n} \frac{(\tau_j - \mu - (\tau_{j-1} - \mu)e^{-\lambda\Delta t_j})^2}{1 - e^{2\lambda\Delta t_j}}. \end{aligned}$$

From the necessary condition for the existence of an extremum

$$\frac{\partial K}{\partial \lambda} = \frac{\partial K}{\partial \mu} = \frac{\partial K}{\partial \eta} = 0,$$

a system of non-linear equations is obtained, from which the maximum likelihood estimates can be solved in the following explicit form

$$\begin{aligned} \widehat{\lambda} &= -\frac{1}{\Delta t} \ln(b_1), \\ \widehat{\mu} &= b_2, \\ \widehat{\eta}^2 &= 2\widehat{\lambda} \frac{b_3}{1 - b_1^2}, \end{aligned}$$

where

$$\begin{aligned} b_1 &= \frac{n \sum_{j=1}^{n} \widetilde{\sigma}_j \widetilde{\sigma}_{j-1} - \sum_{j=1}^{n} \widetilde{\sigma}_j \sum_{j=1}^{n} \widetilde{\sigma}_{j-1}}{n \sum_{j=1}^{n} \widetilde{\sigma}_{j-1}^2 - \big(\sum_{j=1}^{n} \widetilde{\sigma}_{j-1}\big)^2}, \\ b_2 &= \frac{\sum_{j=1}^{n} (\widetilde{\sigma}_j - b_1 \widetilde{\sigma}_{j-1})}{n(1 - b_1)}, \\ b_3 &= \frac{1}{n} \sum_{j=1}^{n} (\widetilde{\sigma}_j - b_1 \widetilde{\sigma}_{j-1} - b_2(1 - b_1))^2, \end{aligned}$$

and $\widetilde{\sigma}_0, \widetilde{\sigma}_1, \dots, \widetilde{\sigma}_n$ are the observations of the process. It should be emphasized that in general explicit estimators do not exist and the estimation is usually done by solving numerically a non-linear algebraic equation system.

4.4. Simulation of the noise part of the stress process

For stochastic differential equations there exist similar numerical solution schemes as for the deterministic equations (Kloeden and

Platen, 1992; Sobczyk, 1991). In the following, we use the simplest possible scheme, the Euler–Maruyama integrator. Let us here recall some basic ideas of the methods. The aim is to construct a numerical approximation of the stochastic differential equation

$$d\boldsymbol{\sigma}(t) = \lambda(\boldsymbol{\mu} - \boldsymbol{\sigma}(t))dt + \boldsymbol{\eta} d\mathbf{W}(t). \tag{12}$$

For notational simplicity, the subscript "n" denoting the noise part of the stress process is omitted above and in the following. If we want to construct a time-discrete approximation of this equation on $0 \le t \le T$, we proceed as in the deterministic case. We split the time interval $0 = t_0 \le t_1 \le \ldots \le t_N = T$ and write $\boldsymbol{\sigma}_k = \boldsymbol{\sigma}(t_k)$. Then the *Euler–Maruyama* method for the stochastic differential Eq. (12) is

$$\boldsymbol{\sigma}_{k+1} = \boldsymbol{\sigma}_k + \lambda(\boldsymbol{\mu} - \boldsymbol{\sigma}_k)(t_{k+1} - t_k) + \boldsymbol{\eta}(\mathbf{W}(t_{k+1}) - \mathbf{W}(t_k))$$

starting from $\boldsymbol{\sigma}_0 = \boldsymbol{\sigma}(0)$. The main difference compared to the deterministic equation is that we need to generate the random increments $\mathbf{W}(t_{k+1}) - \mathbf{W}(t_k)$. In practice, we make it as follows. To simplify notation, the procedure is shown only for a single component of $\mathbf{W}$. It is observed that

$$W(t_{k+1}) - W(t_k) \sim W(t_{k+1} - t_k),$$

which means that both sides of the similitude have the same (normal) distribution $\mathrm{N}(0, t_{k+1} - t_k)$. The classical connection between a normal and the standard normal distribution is $\mathrm{N}(0, t_{k+1} - t_k) = \sqrt{t_{k+1} - t_k}\,\mathrm{N}(0, 1)$, thus for the increment it can be written

$$W(t_{k+1}) - W(t_k) \sim \sqrt{t_{k+1} - t_k} r_k,$$

where r_k has a distribution $\mathrm{N}(0, 1)$. In the numerical implementation, r_k can be computed using a random number generator, which usually delivers $\mathrm{N}(0, 1)$ distributed random numbers.

5. Processing results

In HCF analysis, two different analysis types can be defined, i.e. determination of the finite lifetime when loading exceeds the fatigue limit or computing the safety factor when requiring endurance for an infinite lifetime. These two different analysis types will be considered in the following.

5.1. Finite lifetime

In this case, we define the random lifetime variable T_f by the equation $D(T_\mathrm{f}) = 1$. Thus repeating the solution procedure, say N times for different realizations of the process $\boldsymbol{\sigma}(t)$, we obtain a collection of failure times $T_\mathrm{f}(j)$, where $j = 1, \ldots, N$. The normalized histogram of this collection gives an approximation for the probability density function of T_f.

A model for the distribution of lifetimes has been widely studied, see e.g. Nelson (2004). Usually either the log-normal or the Weibull distribution is used.

5.2. Infinite lifetime on fatigue limit and safety factor

For the case of the infinite lifetime, the natural question is how close a certain design is from it. This distance is measured by a safety factor and its definition in the continuum model is explained next.

Let us look the evolution Eq. (3) for the back-stress $\boldsymbol{\alpha}$ in the case when there exists a stable state $\dot{\boldsymbol{\alpha}} = 0$ for some $t \ge T$. Observing that if $\beta(\boldsymbol{\sigma}(t), \boldsymbol{\alpha}_S; \sigma_{-1}) < 0$, we may "shrink" the surface, i.e. the parameter σ_{-1} such that stresses are still located inside the surface, i.e. $\beta(\boldsymbol{\sigma}(t), \boldsymbol{\alpha}_S; \sigma') < 0$ for $\sigma' < \sigma_{-1}$. The minimal possible value of the parameter σ' is denoted σ^*, and the safety factor can be defined as

$$S = \frac{\sigma_{-1}}{\sigma^*}.$$

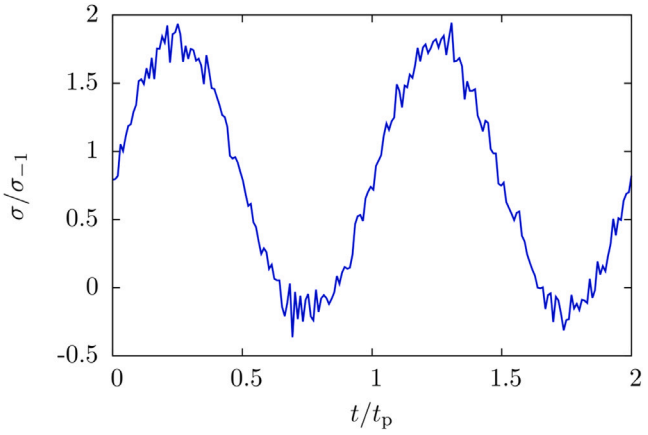

Fig. 5. A realization of a one-dimensional stress history, $\eta = 0.1\sigma_{-1}/\sqrt{t_\mathrm{p}}$.

Physically this means that we can choose for the structure being analysed to have weaker mechanical properties. The safety factor tells us how much weaker the material could be to sustain the loading for infinite life.

If now $\beta(\boldsymbol{\sigma}(t), \boldsymbol{\alpha}_S; \sigma^*) \le M^* < 0$, and $D(T) < 1$, it is easy to see that

$$S = \frac{1}{1 + M^*},$$

where

$$M^* = \max_{t \ge T^*} \beta(\boldsymbol{\sigma}(t), \boldsymbol{\alpha}^*; \sigma_{-1}). \tag{13}$$

The corresponding stable state $\boldsymbol{\alpha}^*$, can be found by the min–max problem

$$\min_{\boldsymbol{\alpha}} \max_{t \ge 0} \beta(\boldsymbol{\sigma}(t), \boldsymbol{\alpha}; \sigma_{-1}), \tag{14}$$
$$\max_{t \ge 0} \beta(\boldsymbol{\sigma}(t), \boldsymbol{\alpha}; \sigma_{-1}) \le 0.$$

This can be solved by the classical penalty method of constrained optimization.

If $\boldsymbol{\sigma}(t)$ is a stochastic process, we need to solve the problem for realizations of the process and we obtain samples for M^*, which is a random variable. See the example in Section 6.2.

6. Examples

In this section, some numerical examples are presented to demonstrate the applicability of the stochastic continuum-based fatigue model. Only a log-normal distribution for random variables will be used.

6.1. Uniaxial cyclic load — finite life

We consider a uniaxial stress process of the form

$$\sigma(t) = \sigma_\mathrm{a} \sin(2\pi t/t_\mathrm{p}) + \sigma_\mathrm{m} + \eta W(t), \tag{15}$$

i.e. a sinusoidal stress history with stationary noise, which is a special case of Ornstein–Uhlenbeck type noise, see Fig. 5. Assuming that the noise is of the form

$$\sigma_\mathrm{n}(t) \sim \eta W(t) \sim \eta \mathrm{N}(0, 1) = \mathrm{N}(0, \eta^2),$$

that is, η^2 is a variance computed from a point-wise sample of the noise. Moreover, $\mathrm{E}(\sigma_n(t)) = 0$. Since the process $\sigma_n(t)$ is assumed to be stationary, the variance and the expected value does not depend on time. Hence, we may compute the preceding estimators from the one realization considering sufficiently many data points. Only the parameter η need be estimated.

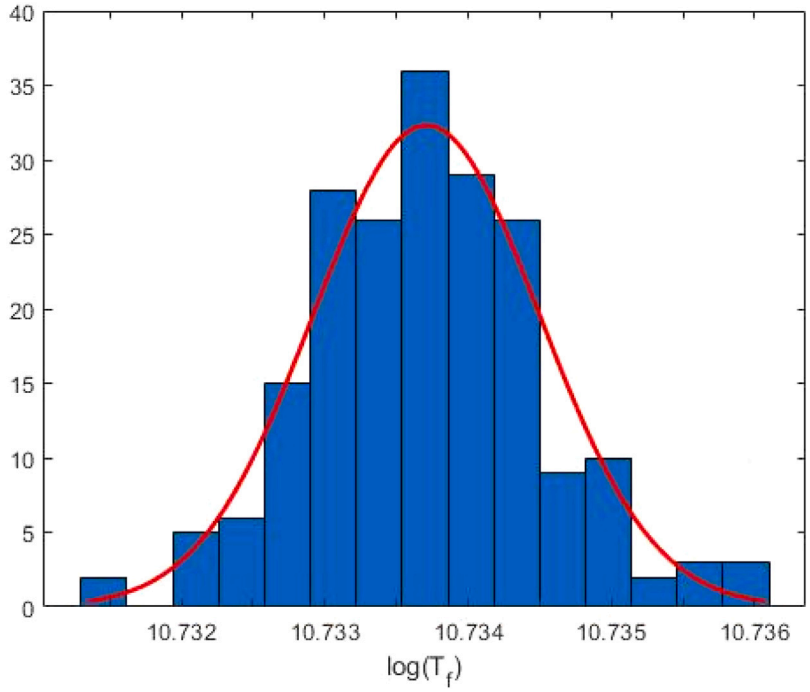

Fig. 6. Histogram approximation for a log-normal distribution of lifetime.

If recorded data $\widetilde{\sigma}(t)$ are of the similar sinusoidal type as (15), we compute realization for the noise by

$$\widetilde{\sigma}_{\mathrm{n}}(t) = \widetilde{\sigma}(t) - \sigma_{\mathrm{a}} \sin(2\pi t/t_{\mathrm{p}}) - \sigma_{\mathrm{m}}$$

and the corresponding estimator for η is $\widehat{\eta}^2 = \mathrm{Var}\{\widetilde{\sigma}_n(t_j) : j = 1, \dots, m\}$, i.e. it is enough to compute the variance of the noisy data.

The material parameters of the model are the same as in Ottosen et al. (2008), i.e.

$$A = 0.225,\ C = 1.25,\ K = 2.65 \times 10^{-5},\ L = 14.4,\ k = 0.$$

For the stress history, the following parameter values are used: $\sigma_{\mathrm{m}} = 0.8\sigma_{-1}$, $\sigma_{\mathrm{a}} = \sigma_{-1}$ and $\eta = 0.1\sigma_{-1}/\sqrt{t_{\mathrm{p}}}$. We obtain an approximation for a logarithmic probability density function of lifetime $\ln(T_{\mathrm{f}})$, see Fig. 6. Here, the fatigue life T_{f} is the same as the cycle number, i.e. $t_{\mathrm{p}} = 1\,\mathrm{s}$. Since the lifetime is log-normally distributed, $\ln(T_{\mathrm{f}}) \sim N(10.7337, 6.239 \cdot 10^{-7})$. From this, the lifetime probabilities can be computed, e.g. the lifetime with 95% probability $T_{95\%}$ can be found from $\mathbb{P}(T_{\mathrm{f}} > T_{95\%}) = 0.95$, giving the result $T_{95\%} = 4.5817 \cdot 10^4$ cycles.

The effect of η-parameter to the fatigue life is demonstrated in Fig. 7. The mean value of 25 realizations decreases with increasing η in the range $(0.005 - 0.1)\sigma_{-1}/\sqrt{t_{\mathrm{p}}}$. The fatigue life is only 22% in comparison to the deterministic case when $\eta = 0.1\sigma_{-1}/\sqrt{t_{\mathrm{p}}}$. Time step used in integration of the evolution has been $\Delta t = 0.01\, t_{\mathrm{p}}$. The standard deviation at specific η value is of the order of 20–70 cycles.

In Figs. 8–9 behaviour of the stochastic model is compared to the deterministic one during the first half-cycle, where the difference is more clearly seen. Quite amazingly the stochastic model shows more quick adaptation to the loading, i.e. the evolution of the $\boldsymbol{\alpha}$-tensor is more rapid than in the deterministic case. This results in a more slow damage evolution at the beginning of the loading process. However, after the transient period the damage evolution for the stochastic case is faster, which is to be expected.

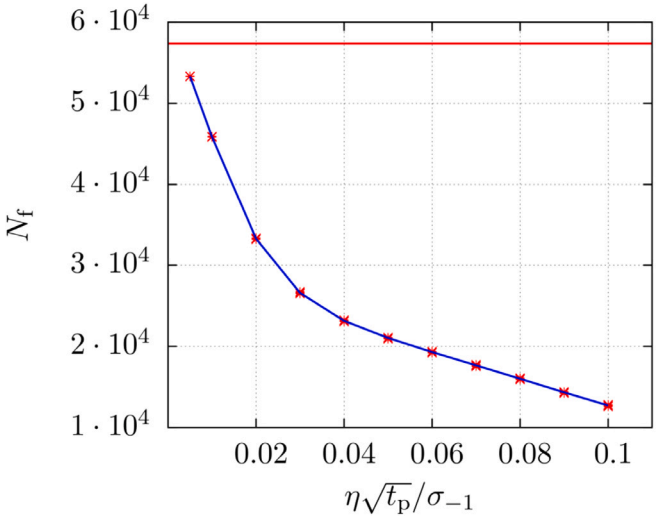

Fig. 7. Fatigue life as a function of η in a uniaxial loading with $\sigma_{\mathrm{m}} = 0.8\sigma_{-1}$ and $\sigma_{\mathrm{a}} = \sigma_{-1}$. The blue line connects the mean values and the red horizontal line shows the deterministic value 57369 cycles, time step $\Delta t = 0.01\, t_{\mathrm{p}}$. (For interpretation of the references to colour in this figure legend, the reader is referred to the web version of this article.)

6.2. Safety factor analysis of a connecting rod

A connecting rod links a piston to a crankshaft. It is one of the most loaded engine components. In particular, high-cycle fatigue calculations are important, as is the ability to make them with stochastic loading, because gas engines have cycle-to-cycle variations in cylinder peak pressure, even though the engine is running a constant load

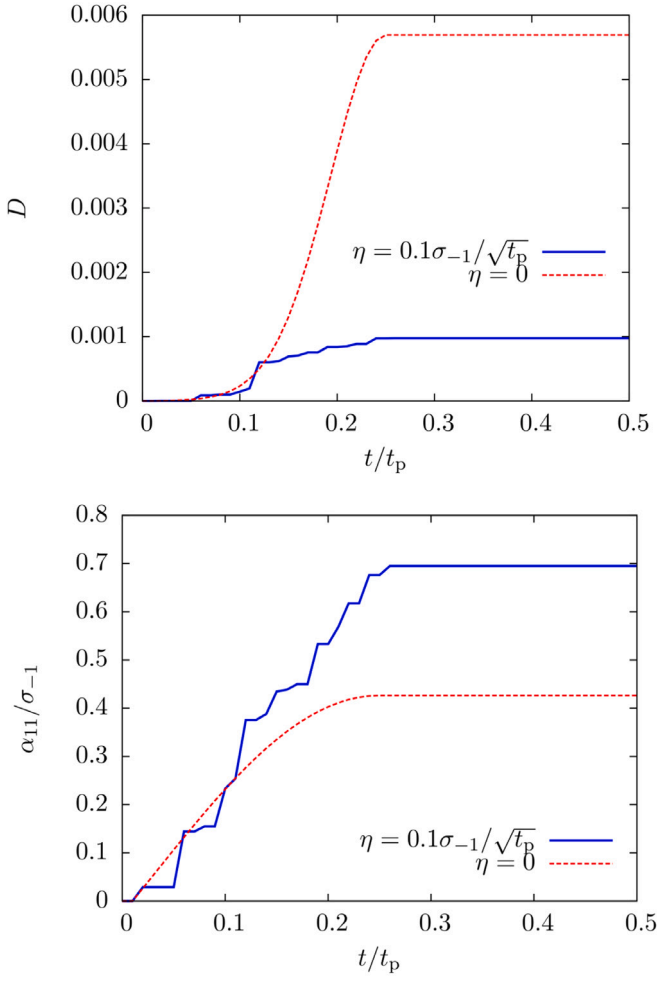

Fig. 8. Damage and back-stress evolution for the cases $\eta = 0.1\sigma_{-1}/\sqrt{t_p}$ and for the deterministic one $\eta = 0$.

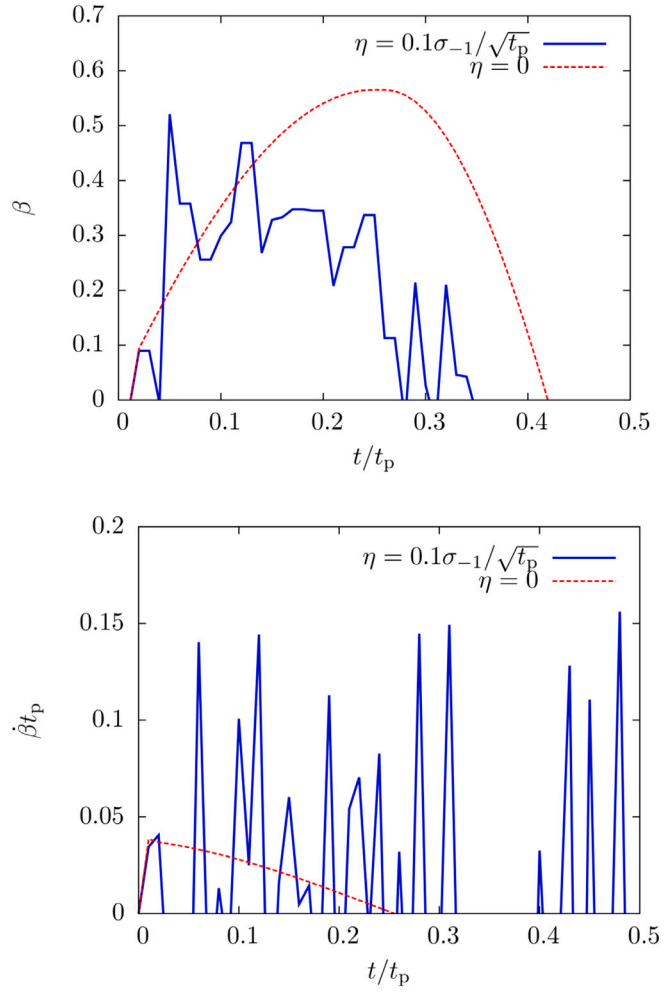

Fig. 9. The endurance surface β and the time rate $\dot{\beta}$. Only positive values shown due to the fact that damage and the $\boldsymbol{\alpha}$-tensor only evolves when $\beta > 0$ and $\dot{\beta} > 0$.

point.[2] In this example, we consider stresses in a connecting rod of a medium speed four stroke engine, see Mäntylä et al. (2017), Göös et al. (2017) for details of the connecting rod calculations. Cylinder pressure histories are recorded from 300 engine cycles and two representative histories are shown in Fig. 10. A critical point from the connecting rod was selected and its stress histories are computed. In Fig. 11, a stress history is shown corresponding to one of the pressure curves shown in Fig. 10.

Every pressure curve corresponds to a stress path in the stress space. We interpret the stress paths as realizations $\{\widetilde{\boldsymbol{\sigma}}_j(t)\}_{j=1}^{300}$, where $-360 \leq t \leq 360$. Time is thus interpreted as the rotation angle of the crankshaft. We compute an asymptotically stable state $\boldsymbol{\alpha}_S^*$ of their mean curve and obtain

$$\widetilde{M}_j^* \approx \beta(\widetilde{\boldsymbol{\sigma}}_j(0), \boldsymbol{\alpha}_S^*; \sigma_{-1}), \quad j = 0, \ldots, 300.$$

The cumulative distribution function of random variable M^*, defined in (13), is given in Leadbetter and Rootzén (1988) by

$$F_M(m) = \begin{cases} \exp(-(-am - b)^c), & \text{when } m < 0, \\ 1, & \text{when } m \geq 0, \end{cases}$$

with parameters $a = 1$, $b = -0.53$ and $c = 17$ (see Fig. 12).

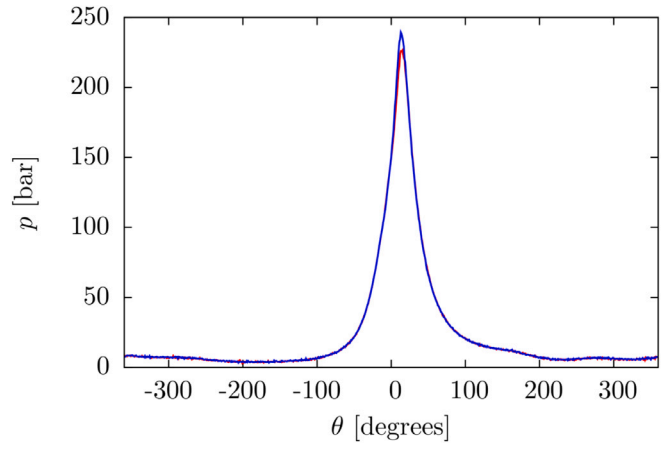

Fig. 10. Measured two extreme cylinder pressure histories.

For example, for the safety factor, $S_{0.95}$, what is obtained with a 95% probability can be computed as follows

$$0.95 = \mathbb{P}\left(S \geq S_{0.95}\right) = \mathbb{P}\left(\frac{1}{M^*+1} \geq S_{0.95}\right) = \mathbb{P}\left(M^* \leq \frac{1}{S_{0.95}} - 1\right).$$

[2] Frondelius et al. (2018) provides a comprehensive review of engine calculations.

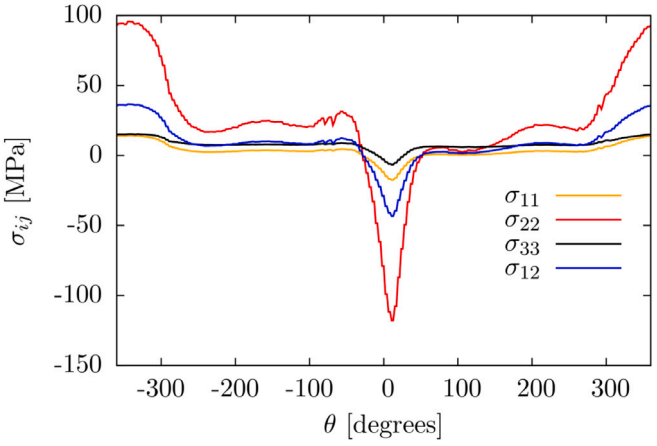

Fig. 11. Example of one computed stress history (minimum pressure curve in Fig. 10 marked in red) in a connecting rod. Stress components σ_{13} and σ_{23} are close to zero, and are thus not shown. (For interpretation of the references to colour in this figure legend, the reader is referred to the web version of this article.)

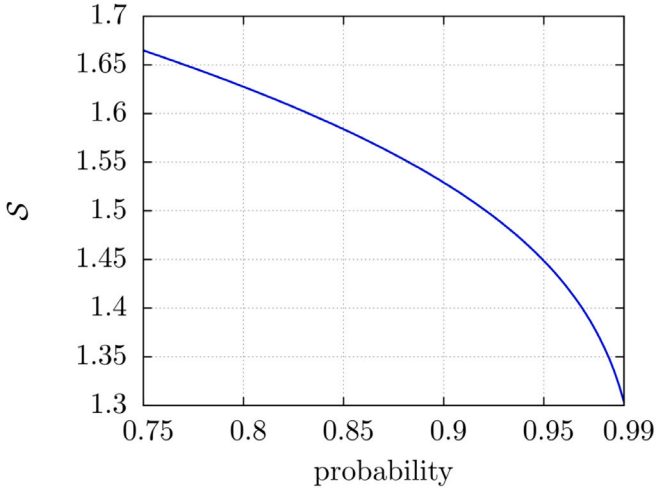

Fig. 13. Safety factor $S = 1/(1 + M^\star)$ as a function of probability.

Then the lower bound of the safety factor can be obtained as

$$m_{0.95} = \frac{1}{S_{0.95}} - 1 \quad \text{thus} \quad S_{0.95} = \frac{1}{m_{0.95} + 1}.$$

Since

$$0.95 = F_M(m_{0.95}) = \exp(-(-m_{0.95} + 0.53)^{17}),$$

we obtain $m_{0.95} = -0.31$ and $S_{0.95} = 1.45$.

The dependency of the safety factor S on probability $\mathbb{P}$ is shown in Fig. 13.

7. Conclusions

In this paper, we extend the (deterministic) continuum model for the high-cycle fatigue (Ottosen et al., 2008) to the case where the stress history is assumed to be a stochastic process. This can be done in a natural way, since the continuum fatigue method is based on differential equations, i.e. the damage accumulation and the movement of the endurance surface are governed by evolution equations written in terms of time rates and not changes per cycle. Moreover, the approach is inherently multiaxial and all stress components are treated in a unified manner.

Here, the stochastic approach is applied in two different tasks relevant to high-cycle fatigue analysis. The first one is related to determining the lifetime when loading is above the fatigue limit but still in the HCF range. Due to stochastic loading, the finite lifetime is a stochastic variable for which the probability distribution can be constructed. The second task governs analysis of the safety factor for infinite life cases. A definition of the safety factor in the continuum-based fatigue analysis method is given, which is related to finding the maximum value of the endurance function for which the probability distribution function can be computed.

Finally, two illustrative examples are presented showing the feasibility of the proposed method.

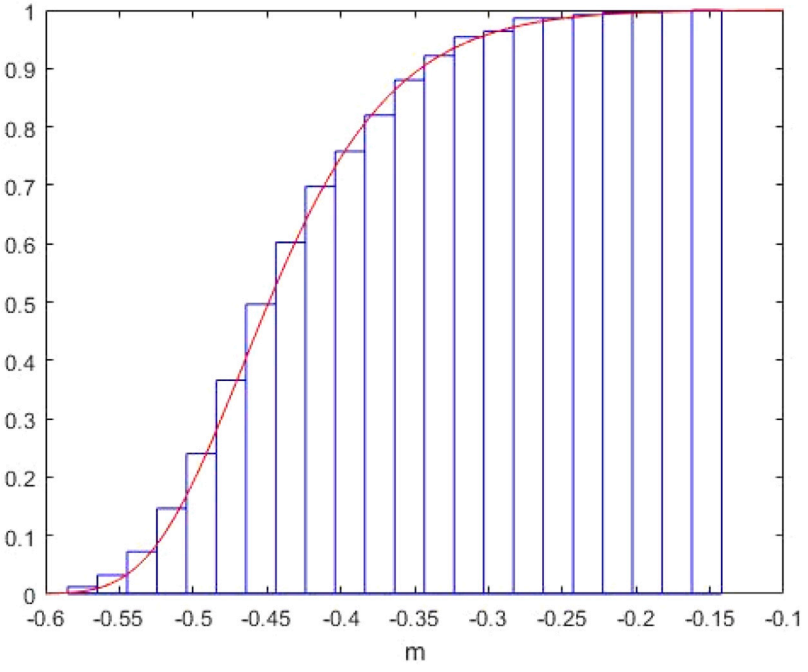

Fig. 12. Cumulative distribution function of $M^\star$, defined in (13).

CRediT authorship contribution statement

Tero Frondelius: Conceptualization, Writing – review & editing, Funding acquisition. **Terhi Kaarakka:** Conceptualization, Methodology, Writing – review & editing. **Reijo Kouhia:** Conceptualization, Writing – review & editing. **Jari Mäkinen:** Conceptualization. **Heikki Orelma:** Conceptualization, Methodology, Software, Validation, Writing – original draft. **Joona Vaara:** Conceptualization, Writing – review & editing.

Declaration of competing interest

The authors declare that they have no known competing financial interests or personal relationships that could have appeared to influence the work reported in this paper.

Acknowledgements

We wish to express our thanks to Professor Simo Särkkä from Aalto University for his consultations and suggestions. He also kindly gave us his forthcoming book (Särkkä and Sulin, 2019) for our use. We would like to thank Lic.Phil. Osmo Kaleva for his comments and suggestions, Dr. Djebar Baroudi for help with the numerical computations and the anonymous reviewers for constructive comments and suggestions to amend the manuscript.

In addition, the authors would like to acknowledge the financial support of Business Finland (former Tekes) in the form of a research project WIMMA Dnro 1566/31/2015, ISA Wärtsilä Dnro 7734/31/2018 and ISA TAU Dnro 7204/31/2018.

References

Abdul-Latif, A., 2021. Continuum damage model for low-cycle fatigue of metals: An overview. Int. J. Damage Mech. 30 (7), 1036–1078. http://dx.doi.org/10.1177/1056789521991620.

Banvillet, A., Łagoda, T., Macha, E., Niesłony, A., Palin-Luc, T., Vittori, J.-F., 2004. Fatigue life under non-gaussian random loading from various models. Int. J. Fatigue 26 (4), 349–363. http://dx.doi.org/10.1016/j.ijfatigue.2003.08.017.

Böhm, J., Heckel, K., 1982. Die vorhersage der dauerschwingfestigkeit unter berücksichtigung des statistischen größeneinflusses. Mater.wiss. Werkst.tech. 13 (4), 120–128. http://dx.doi.org/10.1002/mawe.19820130408.

Bolotin, V., 1999. Mechanics of Fatigue. In: CRC Mechanical Engineering Series, CRC Press, Boca Raton.

Bomas, H., Linkewitz, T., Mayr, P., 1999. Application of a weakest-link concept to the fatigue limit of the bearing steel sae 52100 in a bainitic condition. Fatigue Fract. Eng. Mater. Struct. 22 (9), 733–741. http://dx.doi.org/10.1046/j.1460-2695.1999.t01-1-00211.x.

Brighenti, R., Carpinteri, A., Corbari, N., 2013. Damage mechanics and Paris regime in fatigue life assessment of metals. Int. J. Press. Vessels Pip. 104, 57–68. http://dx.doi.org/10.1016/j.ijpvp.2013.01.005.

Brighenti, R., Carpinteri, A., Vantadori, S., 2012. Fatigue life assessment under a complex multiaxial load history: an approach based on damage mechanics. Fatigue Fract. Eng. Mater. Struct. 35 (2), 141–153. http://dx.doi.org/10.1111/j.1460-2695.2011.01600x.

Carpinteri, A., Fortese, G., Ronchei, C., Scorza, D., Spagnoli, A., Vantadori, S., 2016. Fatigue life evaluation of metallic structures under multiaxial random loading. Int. J. Fatigue 90, 191–199. http://dx.doi.org/10.1016/j.ijfatigue.2016.05.007.

Chaboche, J., Lesne, P., 1988. A non-linear continuous fatigue damage model. Fatigue Fract. Eng. Mater. Struct. 11 (1), 1–17. http://dx.doi.org/10.1111/j.1460-2695.1988.tb01216.x.

Cristofori, A., Benasciutti, D., Tovo, R., 2011. A stress invariant based spectral method to estimate fatigue life under multiaxial random loading. Int. J. Fatigue 33 (7), 887–899. http://dx.doi.org/10.1016/j.ijfatigue.2011.01.013.

Desmorat, R., Kane, A., Seyedi, M., Sermage, J., 2007. Two scale damage model and related numerical issues for thermo-mechanical high cycle fatigue. Eur. J. Mech. A Solids 26 (6), 909–935. http://dx.doi.org/10.1016/j.euromechsol.2007.01.002.

Flaceliere, L., Morel, F., 2004. Probabilistic approach in high-cycle multiaxial fatigue: volume and surface effects. Fatigue Fract. Eng. Mater. Struct. 27 (12), 1123–1135. http://dx.doi.org/10.1111/j.1460-2695.2004.00823.x.

Frondelius, T., Tienhaara, H., Haataja, M., 2018. History of structural analysis & dynamics of Wärtsilä medium speed engines. Rakenteiden Mek. 51 (2), 1–31. http://dx.doi.org/10.23998/rm.69735.

Gardiner, C.W., 1997. Handbook of Stochastic Methods. Springer, New York.

Göös, J., Leppänen, A., Mäntylä, A., Frondelius, T., 2017. Large bore connecting rod simulations. Rakenteiden Mek. 50 (3), 275–278. http://dx.doi.org/10.23998/rm.64658.

Grilli, N., Janssens, K.G., Van Swygenhoven, H., 2015. Crystal plasticity finite element modelling of low cycle fatigue in fcc metals. J. Mech. Phys. Solids 84, 424–435. http://dx.doi.org/10.1016/j.jmps.2015.08.007.

Holopainen, S., Kouhia, R., Könnö, J., Saksala, T., 2016a. Computational modelling of transversely isotropic high-cycle fatigue using a continuum based model. Procedia Struct. Integr. 2, 2718–2725. http://dx.doi.org/10.1016/j.prostr.2016.06.339.

Holopainen, S., Kouhia, R., Saksala, T., 2016b. Continuum approach for modeling transversely isotropic high-cycle fatigue. Eur. J. Mech. A Solids 60, 183–195. http://dx.doi.org/10.1016/j.euromechsol.2016.06.007.

James, J., Webber, N., 2000. Interest Rate Modelling. Wiley.

Kaleva, O., Orelma, H., 2021. Modeling stress history as a stochastic process. Int. J. Fatigue 143, 105996. http://dx.doi.org/10.1016/j.ijfatigue.2020.105996.

Kalluri, S., Bonacuse, P., 2000. Cumulative axial and torsional fatigue: An investigation of load-type sequencing effects. In: Kalluri, S., Bonacuse, P. (Eds.), Multiaxial Fatigue and Deformation: Testing and Prediction. ASTM International, West Conshohocken, PA, pp. 281–301. http://dx.doi.org/10.1520/STP13510S.

Kloeden, P., Platen, E., 1992. Numerical Solution of Stochastic Differential Equations, Vol. 23. In: Applications of Mathematics, Springer-Verlag, Berlin.

Kratz, M.F., 2006. Level crossings and other level functionals of stationary Gaussian processes. Probab. Surv. 3, 230–288. http://dx.doi.org/10.1214/154957806000000087.

Leadbetter, M., Rootzén, H., 1988. Extremal theory for stochastic processes. Ann. Probab. 16 (2), 431–478.

Lemaitre, J., Desmorat, R., 2005. Engineering Damage Mechanics, Ductile, Creep, Fatigue and Brittle Failures. Springer-Verlag, Berlin, Heidelberg.

Lilja, M., Karsson, J., A.Jonsson, Hilding, D., Lindström, S., Leidermark, D., Schmidt, P., 2020. Incremental damage model for fatigue life assessment in complete machinery simulation. In: 16th International LS-DYNA Users Conference. URL https://www.dynalook.com/conferences/16th-international-ls-dyna-conference/constitutive-modeling-t7-1/t7-1-c-constitutive-modeling-106.pdf.

Lindgren, G., 2013. Stationary Stochastic Processes: Theory and Applications. In: Chapman & Hall/CRC Texts in Statistical Science Series, CRC Press, Boca Raton, Florida.

Lindström, S.B., 2020. Continuous-time, high-cycle fatigue model for nonproportional stress with validation for 7075-t6 aluminum alloy. Int. J. Fatigue 140, 105839. http://dx.doi.org/10.1016/j.ijfatigue.2020.105839.

Lindström, S.B., Thore, C.-J., Suresh, S., Klarbring, A., Continuous-time, 2020. High-cycle fatigue model: Validity range and computational acceleration for cyclic stress. Int. J. Fatigue 136, 105582. http://dx.doi.org/10.1016/j.ijfatigue.2020.105582.

Liu, Y., Mahadevan, S., 2007. Stochastic fatigue damage modeling under variable amplitude loading. Int. J. Fatigue 29 (6), 1149–1161. http://dx.doi.org/10.1016/j.ijfatigue.2006.09.009.

Manonukul, A., Dunne, F.P.E., 2004. High- and low-cycle fatigue crack initiation using polycrystal plasticity. Proc. R. Soc. Lond. Ser. A Math. Phys. Eng. Sci. 460 (2047), 1881–1903. http://dx.doi.org/10.1098/rspa.2003.1258.

Mäntylä, A., Göös, J., Leppänen, A., Frondelius, T., 2017. Large bore engine connecting rod fretting analysis. Rakenteiden Mek. 50 (3), 239–243. http://dx.doi.org/10.23998/rm.64914.

Mareau, C., Cuillerier, D., Morel, F., 2013. Experimental and numerical study of the evolution of stored and dissipated energies in a medium carbon steel under cyclic loading. Mech. Mater. 60, 93–106. http://dx.doi.org/10.1016/j.mechmat.2013.01.011.

Mareau, C., Morel, F., 2019. A continuum damage mechanics-based approach for the high cycle fatigue behavior of metallic polycrystals. Int. J. Damage Mech. 28 (6), 838–856. http://dx.doi.org/10.1177/1056789518795204.

Murakami, Y., 2002. Metal Fatigue,Effects of Small Defects and Nonmetallic Inclusions. Elsevier Science.

Nelson, W., 2004. Accelerated Testing. Wiley.

Nguyen, Q.-S., 2003. On shakedown analysis in hardening plasticity. J. Mech. Phys. Solids 51 (1), 101–125. http://dx.doi.org/10.1016/S0022-5096(02)00058-3.

Ottosen, N.S., Ristinmaa, M., Kouhia, R., 2018. Enhanced multiaxial fatigue criterion that considers stress gradient effects. Int. J. Fatigue 116, 128–139. http://dx.doi.org/10.1016/j.ijfatigue.2018.05.024.

Ottosen, N., Stenström, R., Ristinmaa, M., 2008. Continuum approach to high-cycle fatigue modeling. Int. J. Fatigue 30 (6), 996–1006. http://dx.doi.org/10.1016/j.ijfatigue.2007.08.009.

Pfanzagl, J., 1994. Parametric Statistical Theory. De Gruyter.

Polizzotto, C., Borino, G., Fuschi, P., 2001. Weak forms of shakedown for elastic–plastic structures exhibiting ductile damage. Meccanica 36, 49–66. http://dx.doi.org/10.1023/A:1011969520565.

Portugal, I., Olave, M., Urresti, I., Zurutuza, A., López, A., Muñiz Calvente, M., Fernández-Canteli, A., 2019. A comparative analysis of multiaxial fatigue models under random loading. Eng. Struct. 182, 112–122. http://dx.doi.org/10.1016/j.engstruct.2018.12.035.

Särkkä, S., Sulin, A., 2019. Applied Stochastic Differential Equations. Cambridge University Press, http://dx.doi.org/10.1017/9781108186735.

Sobczyk, K., 1991. Stochastic Differential Equations. with Applications to Physics and Engineering, Vol. 40. In: Mathematics and its Applications. East European Series, Kluwer Academic Publishers Group, Dordrecht.

Suresh, S., 1998. Fatigue of Materials, 2nd Edition Cambridge University Press.

Suresh, S., Lindström, S., Thore, C.-J., Klarbring, A., 2021. Topology optimization for transversely isotropic materials with high-cycle fatigue as a constraint. Struct. Multidiscip. Optim. 63, 161–163. http://dx.doi.org/10.1007/s00158-020-02677-2.

Suresh, S., Lindström, S., Thore, C.-J., Torstenfelt, B., Klarbring, A., 2020. Topology optimization using a continuous-time high-cycle fatigue model. Struct. Multidiscip. Optim. 61, 1011–1025. http://dx.doi.org/10.1007/s00158-019-02400-w.

Vaara, J., Mäntylä, A., Frondelius, T., 2017. Brief review on high-cycle fatigue with focus on non-metallic inclusions and forming. Rakenteiden Mek. 50 (3), 146–152. http://dx.doi.org/10.23998/rm.65048.

Wei, H., Carrion, P., Chen, J., Imanian, A., Shamsaei, N., Iyyer, N., Liu, Y., 2020. Multiaxial high-cycle fatigue life prediction under random spectrum loadings. Int. J. Fatigue 134, 105462. http://dx.doi.org/10.1016/j.ijfatigue.2019.105462.

Weibull, W., 1939. A statistical theory of strength of materials, IVB-Handl. No 151.

Wormsen, A., Sjödin, B., Härkegård, G., Fjeldstad, A., 2007. Non-local stress approach for fatigue assessment based on weakest-link theory and statistics of extremes. Fatigue Fract. Eng. Mater. Struct. 30 (12), 1214–1227. http://dx.doi.org/10.1111/j.1460-2695.2007.01190.x.

Zhang, L., Zhao, L., Jiang, R., Bullough, C., 2020. Crystal plasticity finite-element modelling of cyclic deformation and crack initiation in a nickel-based single-crystal superalloy under low-cycle fatigue. Fatigue Fract. Eng. Mater. Struct. 43 (8), 1769–1783. http://dx.doi.org/10.1111/ffe.13228.